

Squint: Fast Visual Reinforcement Learning for Sim-to-Real Robotics

Abdulaziz Almuzairee¹ Henrik I. Christensen¹

<https://aalmuzairee.github.io/squint>

Task	Reach Cube	Reach Can	Lift Cube	Lift Can	Place Cube	Place Can	Stack Cube	Stack Can
Start								
Success								
Time	2 minutes	2 minutes	3 minutes	4 minutes	5 minutes	6 minutes	6 minutes	9 minutes

Fig. 1. **Fast Sim-to-Real Robotics.** We setup 8 visual tasks on the 5 DoF SO-101 Robotics Arm in ManiSkill3 and train our method, *Squint*, purely from images and proprioceptive state on these tasks for 15 minutes. After 15 minutes, we take the final checkpoint, and deploy it zero-shot to our real robot setup. We show visuals of the real robot for each of the tasks above, along with an image of the "Start" frame, the final "Success" frame, and the "Time" it takes our agent to converge in simulation for each task on a single 3090 RTX GPU.

Abstract—Visual reinforcement learning is appealing for robotics but expensive – off-policy methods are sample-efficient yet slow; on-policy methods parallelize well but waste samples. Recent work has shown that off-policy methods can train faster than on-policy methods in wall-clock time for state-based control. Extending this to vision remains challenging, where high-dimensional input images complicate training dynamics and introduce substantial storage and encoding overhead. To address these challenges, we introduce Squint, a visual Soft Actor Critic method that achieves faster wall-clock training than prior visual off-policy and on-policy methods. Squint achieves this via parallel simulation, a distributional critic, resolution squinting, layer normalization, a tuned update-to-data ratio, and an optimized implementation. We evaluate on the SO-101 Task Set, a new suite of eight manipulation tasks in ManiSkill3 with heavy domain randomization, and demonstrate sim-to-real transfer to a real SO-101 robot. We train policies for 15 minutes on a single RTX 3090 GPU, with most tasks converging in under 6 minutes.

I. INTRODUCTION

Visual reinforcement learning (RL) [51] offers a compelling paradigm for robotics — enabling deployment onto real robots with camera inputs and requiring no task-specific instrumentation [37, 85, 38]. Despite this appeal, training visuomotor

policies remains notoriously expensive, demanding millions of environment interactions and substantial compute.

Over the past few years, researchers have made strides in reducing the number of environment interactions needed, often referred to as sample efficiency, by improving off-policy algorithms. These off-policy algorithms, such as SAC [24], TD3 [19], and TD-MPC2 [27], reuse experiences through a replay buffer. Yet, these improvements come with computational costs that increase training wall-time of these agents in simulation. This slows research iteration. On the other hand, on-policy methods like Proximal Policy Optimization [63] offer poor sample efficiency, without any experience reuse, but can parallelize trivially across thousands of environments on modern GPUs, achieving faster wall-times than their off-policy counterparts. This has led to on-policy dominance in GPU-accelerated simulators and PPO to be the de facto standard for sim-to-real robotics in the past decade [30, 35].

While sample efficiency and wall-time are both important axes for reinforcement learning, recent works like FastTD3 and FastSAC [65, 64] explore an intermediate axis, one where off-policy algorithms can be tuned to maximize wall-time rather than sample efficiency, achieving faster wall times than their on-policy counterparts in parallelized simulations. These works made significant progress in scaling off-policy learning

¹University of California San Diego. Correspondence to: Abdulaziz Almuzairee <aalmuzairee@ucsd.edu>.

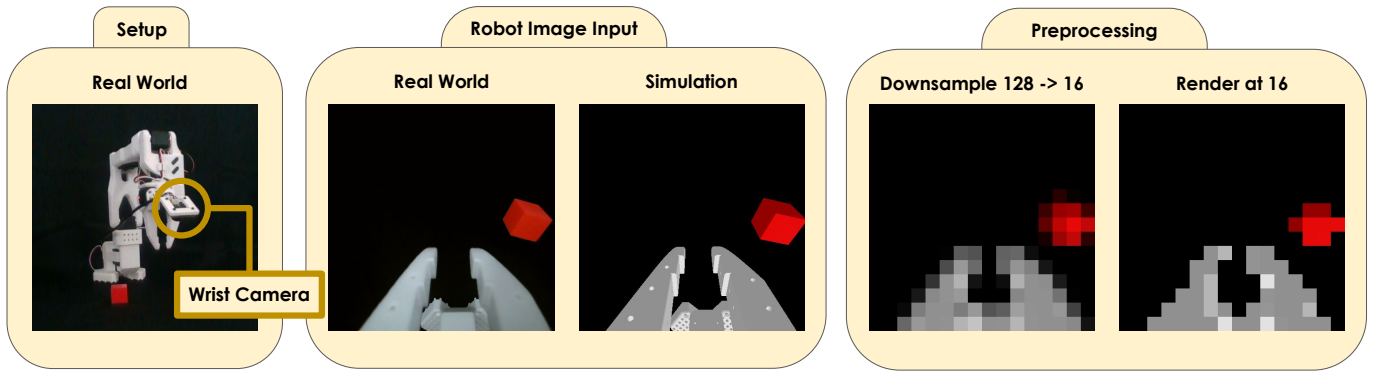


Fig. 2. **Robot Setup.** (Left) Setup of the real robot from an external camera. (Middle) The input camera image for the robot in both the real world and simulation. We only use the wrist camera as the input image for the robot. (Right) We display different preprocessing effects, downsampling from a higher resolution vs rendering at the target resolution directly.

for state-based control. Yet, extending these works to visual reinforcement learning remains nontrivial: high-dimensional input images complicate training dynamics, storing them in replay buffers strains memory, and encoding them through convolutional networks adds computational overhead.

Motivated by these challenges, we introduce our method, *Squint*, a visual based Soft Actor Critic method, that through careful image preprocessing, architectural design choices, and hyperparameter selection, is able to leverage parallel environments and experience reuse effectively, achieving faster wall-clock training time than both prior visual off-policy and on-policy methods, and solving visual robotic tasks in minutes.

To train *Squint*, we leverage ManiSkill3 [70], a fast-GPU simulator, with powerful batched rendering capabilities, and create a digital twin of our real robot setup. Our real robot setup consists of a 5 DoF SO-101 Robot Arm [10]. We build 8 distinct tasks, which we term the *SO-101 Task set*, and use them as a testbed for investigating scalable visual reinforcement learning. We train our method and baselines on the SO-101 Task set for 15 minutes, and deploy them to our real robot setup, which can be seen in Figure 1 and Figure 2.

Our key contributions are (1) *Squint*: A fast off-policy visual actor critic method that achieves faster wall-clock training than prior visual RL methods, with extensive experiments justifying each design choice. (2) SO-101 Task Set: eight manipulation tasks in ManiSkill3 with heavy domain randomization for sim-to-real transfer. (3) Real-world validation: Policies trained in 15 minutes on a single RTX 3090, deployed zero-shot to the real world SO-101 hardware.

II. RELATED WORK

Parallel Simulators for Robotics. Simulators provide a fast way for reinforcement learning agents to learn in a safe, constrained environments [7, 13]. Early parallelization in CPU allowed agent to train faster in terms of wall time [30, 71, 37, 80, 84]. With the advent of fast GPU-based parallelization, these simulators became faster, and allowed

the community to iterate faster on training and deployment. [46, 50, 53, 23, 70, 66, 83] Most notably, ManiSkill3 [70] provides fast GPU-based batched rendering, which allows researchers to train fast visual based reinforcement learning agents for deployment. Due to its realism, and ease of use, we use ManiSkill3 as our main simulator for this work. Despite its realism, domain randomization [73] is necessary to bridge the sim-to-real gap. Thus, we apply domain randomization to our task set to allow better sim to real transfer.

Visual Reinforcement Learning. Learning from vision has driven the start of deep RL in the recent decade [51, 52]. Building on it, many works explored different methods to improve off-policy training sample efficiency, including: autoencoder architectures [17, 77], contrastive learning representations [69], data regularized representations [41, 78], and model-based representations [25, 27, 20]. Perhaps most notably, DrQ-v2 [78] is widely used as a solid baseline for visual reinforcement learning sample efficiency. Unfortunately, this sample efficiency comes at the cost of training wall-time, which on-policy PPO [63] exceeds at in scale. While most prior visual off policy learning algorithms focus on sample efficiency, we follow PQL[44], PQN [21], FastTD3 [65] and FastSAC [64] in focusing on training wall-time, and introduce our algorithm, *Squint*, to excel at this axis in the visual RL domain.

III. BACKGROUND

Visual Reinforcement Learning formulates the interaction between the agent and the environment as a Partially Observable Markov Decision Process (POMDP) [36], defined by a tuple of $(\mathcal{S}, \mathcal{O}, \mathcal{A}, \mathcal{T}, R, \gamma)$. In a POMDP, $s \in \mathcal{S}$ is the state space, $o \in \mathcal{O}$ is the observation space, $a \in \mathcal{A}$ the action space, $\mathcal{T} : \mathcal{S} \times \mathcal{A} \times \mathcal{S} \rightarrow [0, 1]$ is the state-to-state transition probability function, $R : \mathcal{S} \times \mathcal{A} \rightarrow \mathbb{R}$ is the reward function and γ is the discount factor. At each time step t , the agent receives as input: a single RGB image as an observation $o \in \mathcal{O}$ and *optionally* the proprioceptive state $s^{proprio} \in \mathcal{S}$, and is

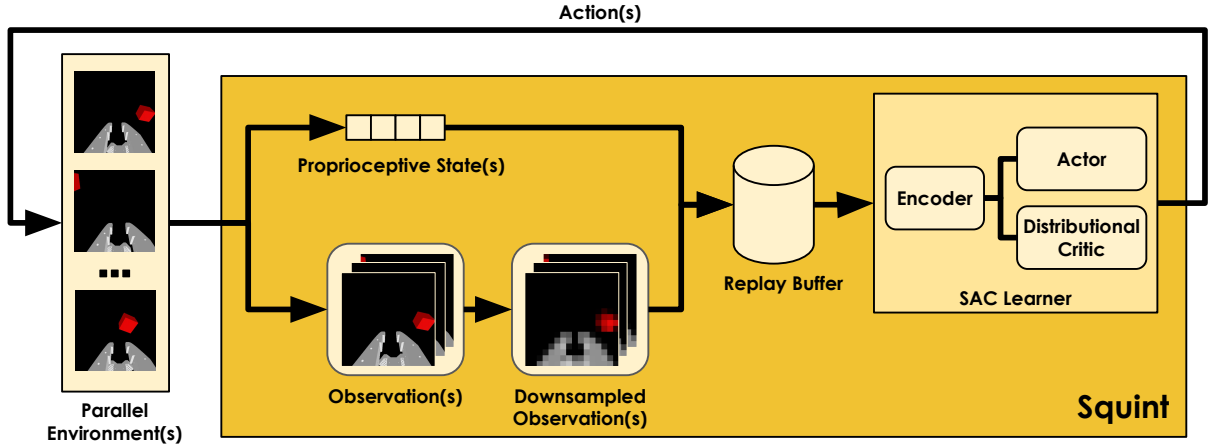


Fig. 3. **Method Diagram.** Squint is a fast off-policy actor-critic visual reinforcement learning algorithm that accelerates training speed by leveraging parallel environments and downsampling input image observations.

queried to select an action a . The goal is to learn a policy $\pi : \mathcal{O} \rightarrow \mathcal{A}$ that maximizes the expected discounted sum of rewards $\mathbb{E}_{\pi}[\sum_{t=0}^{\infty} \gamma^t r_t]$ where $r_t = R(s_t, a_t)$.

Soft Actor Critic (SAC) [24] is an off-policy actor critic algorithm, commonly used for continuous control. SAC concurrently learns a Q-function Q_{θ} (critic) and a policy π_{ϕ} (actor) with a separate neural network for each. The Q-function Q_{θ} aims to estimate the optimal soft state-action value function by minimizing the one step Bellman Residual:

$$y = r_t + \gamma \left(Q_{\bar{\theta}}(s_{t+1}, \tilde{\mathbf{a}}_{t+1}) - \alpha \log \pi_{\phi}(\tilde{\mathbf{a}}_{t+1} | s_{t+1}) \right) \quad (1)$$

$$\mathcal{L}_{Q_{\theta}}(\mathcal{D}) = \mathbb{E}_{(s_t, \mathbf{a}_t, r_t, s_{t+1}) \sim \mathcal{D}} \left[(Q_{\theta}(s_t, \mathbf{a}_t) - y)^2 \right] \quad (2)$$

where \mathcal{D} is the replay buffer, $\tilde{\mathbf{a}}_{t+1} \sim \pi_{\phi}(\cdot | s_{t+1})$, $Q_{\bar{\theta}}$ represents an exponential moving average of the weights from Q_{θ} , and α is the temperature parameter [75, 47, 24]. SAC also employs clipped double-Q learning [29, 19] which we omit from our notation for simplicity. The policy π_{ϕ} is a stochastic policy that aims to maximize both entropy and Q-values:

$$\mathcal{L}_{\pi_{\phi}}(\mathcal{D}) = \mathbb{E}_{s_t \sim \mathcal{D}} [\alpha \log \pi_{\phi}(\tilde{\mathbf{a}}_t | s_t) - Q_{\theta}(s_t, \tilde{\mathbf{a}}_t)] \quad (3)$$

where $\tilde{\mathbf{a}}_t \sim \pi_{\phi}(\cdot | s_t)$. The temperature parameter α can either be fixed or learned by minimizing against a target entropy $\mathcal{H}^{\text{target}}$ [24]. Both the critic and actor losses are updated iteratively using stochastic gradient descent in an aim to maximize the expected discounted sum of rewards.

When learning from images, the SAC agent does not have access to state s_t but rather observation \mathbf{o}_t . We follow DrQ and DrQ-v2 [40, 78] in encoding \mathbf{o}_t with a single shared CNN encoder f_{ψ} , such that all previous state inputs s_t can be replaced with $[f_{\psi}(\mathbf{o}_t)]$ or $[f_{\psi}(\mathbf{o}_t), s_t^{\text{proprio}}]$ when proprioceptive state is available. The encoder f_{ψ} is trained end-to-end by the critic gradients.

IV. METHOD

We present *Squint*, a visual Soft Actor Critic [24] method that trains successfully within minutes through: parallel simulation, a distributional critic [8], resolution squinting, layer normalization [4], tuned update-to-data ratio, and an optimized implementation. These trained policies transfer zero-shot to a real-world SO-101 robotic arm. We present the flow of our training pipeline in Figure 3. We further show the impact of each design choice in Figure 4 and discuss them below:

Update-to-Data Ratio. Tuning the update-to-data (UTD) ratio has long been a tradeoff between sample efficiency and training wall time [14]. For minimizing training wall time, prior work has shown that one needs to use a very large number of parallel environments with a very low number of updates [67, 65, 64], creating a low UTD ratio. In Figure 4, we study the impact of these choices, and find that a large number of parallel environments (1024) along with a large number of updates (256) can reduce training time significantly. These findings indicate that while very low UTD ratios (<0.06) work for humanoids [65, 64], manipulation domains seem to benefit from larger UTD ratios, seemingly (0.25) in our task set.

Batch Size. While larger batch sizes have been shown to improve training efficiency in [65, 64], we find that using a lower batch size of 512 provides the same stable training efficiency, while minimizing wall time for every update.

Pytorch Optimizations. Our codebase builds on LeanRL and CleanRL [34]. We add support for both PyTorch compile and cudagraphs [58], which leverage kernel fusion and reduced CPU launch overhead to significantly accelerate the training loop. We further add AMP bfloat16 support for the update loops, reducing training time with convolutional neural networks. Combined, these optimizations give more than a 5x speedup in training speed.

Critic Design Choices. We adopt a Distributional C51 Critic [8], similar to [44, 65, 64], where we minimize cross entropy loss rather than the mean square error on TD-targets. We

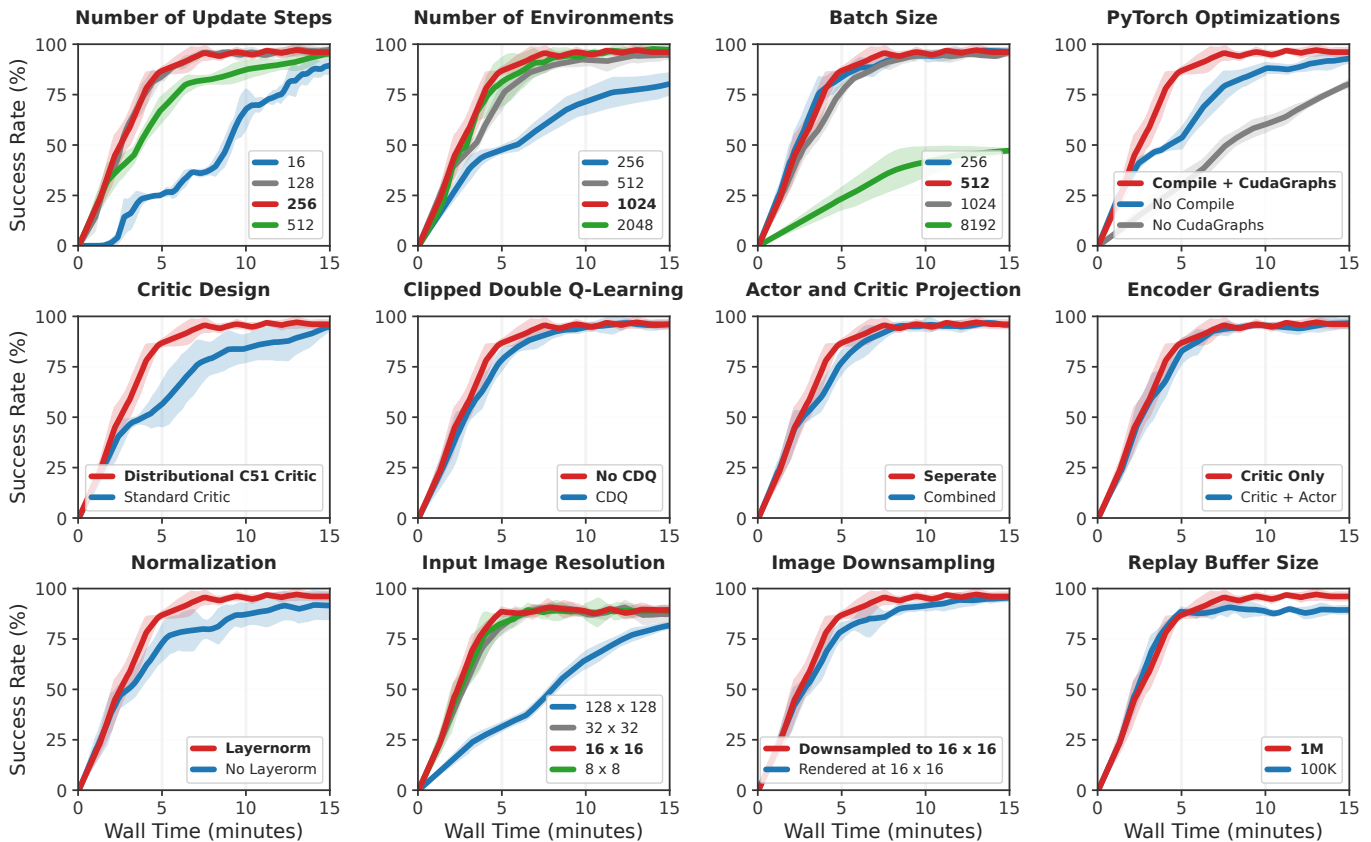


Fig. 4. **Design Choices.** We experiment with the most critical design choices that allow our agents to be trained while maximizing wall-time for sim-to-real robotics deployment. Mean Success Rate and 95% CI over 5 seeds for all 8 tasks.

find that the choice of a distributional critic greatly improves wall time speed, even though it requires more computation than a standard Critic. We further investigate the effect of Clipped Double Q-learning (CDQ) [18] and find a slight improvement in using the average rather than CDQ.

Encoder Design Choices. We leverage a small two layer CNN encoder, and share it between the actor and critic. The encoder is only updated by the critic’s TD-loss. After encoding the images, we pass them through separate one layer projections for each of the actor and critic. We adopt these design choices following prior state-of-the-art visual RL methods [40, 78], though our ablations reveal they yield negligible performance gains on our task set.

Normalization. All our linear layers are followed by Layer Normalization layers [4], which we find to improve training speed, similar to the findings of [5, 55, 64].

Input Image Resolution. We compare training agents with larger and lower input image resolutions, and find them to achieve identical sample efficiency, but varying wall time training speed. We only show the wall time axis in Figure 4. Our findings show that the smaller the resolution, the faster the wall time, and thus we use a 16 x 16 input image resolution.

Squinting. We compare rendering at 16 x 16 vs rendering at a high resolution of 128 x 128 and then area downsampling

to 16 x 16, which we refer to as *squinting*. We find that downsampling improves performance on our task set. This downsampling provides natural anti-aliasing and preserves scene structure, which we hypothesize aids sim-to-real transfer. We further show a visual comparison in Figure 2.

Replay Buffer Size. Due to our use of squinting and low image sizes of 16 x 16, we are able to scale replay buffer size to easily fit on the GPU for faster training speed. We compare using 100K vs 1M replay buffer storage size, and find that the 1M improves asymptotic method success rate on our task set by 7%. While we use a simple FIFO buffer, we leave it to future work to use more advanced buffer sampling techniques [62, 31] that could further improve wall time.

Simulation Control Frequency. To facilitate faster training times, we train with 10Hz control frequency using a PD Joint Position Target Delta controller. We use large position offset limits, to allow the agent to move faster in simulation.

Real-World Robot Transfer. To transfer trained agents to the real robot, without compromising safety, we scale all actions down by 0.15, and triple the control frequency to 30Hz. While this constitutes a mismatch between simulation and real world control frequency, we find that a higher control frequency in the real world provides faster recovery control for the robot, and provides smoother trajectories.

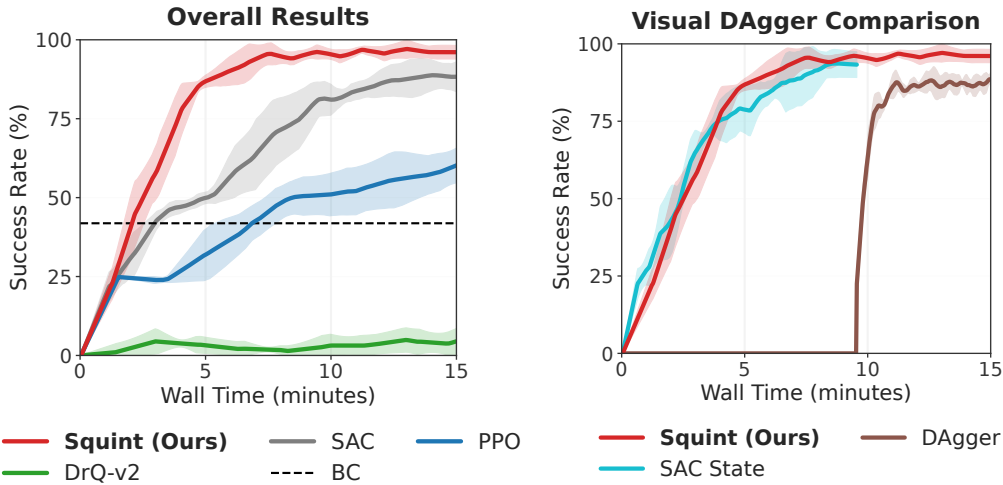


Fig. 5. **Overall Results.** (Left) Comparison with visual RL baselines. (Right) Comparison with State-to-Visual DAgger, where we include the time it takes to train an SAC state expert into the comparison. Mean Success Rate and 95% CI over 5 seeds on all tasks.

V. EXPERIMENTS

We setup 8 distinct tasks in ManiSkill3 [70] simulator with the 5-DoF SO-101 robotic arm [10], and train our method and baselines on each of these tasks for 15 minutes over 5 seeds. We only use the wrist camera image and proprioceptive state as input. We then deploy the best seed from each method on each task, and evaluate it zero-shot on our real world robot setup. Our real robot setup is shown in Figure 2.

Task Design. We design the tasks to be digital twins of the real world setup, thereby reducing the visual gap. We use the wrist camera for learning, as it has been shown to provide better representations than third person cameras in robot manipulation [32, 2]. For each task in our task set, the objects are randomly placed on the table in a 0.2m x 0.2m xy box around the gripper’s starting xy position. The tasks are: (1) *Reach Cube*: robot reaches 2 cm above the cube. (2) *Reach Can*: robot reaches 2 cm above the can. (3) *Lift Cube*: robot lifts the cube and moves to a predefined rest position. (4) *Lift Can*: robot lifts the can and moves to a predefined rest position. (5) *Place Cube*: robot lifts the cube and places it into the container. (6) *Place Can*: robot lifts the can and places it into the container. (7) *Stack Cube*: robot lifts the red cube and stacks it on top of the blue cube. (8) *Stack Can*: robot lifts the cube and stacks it on top of the can. We show the start and success position of each task in Figure 1.

Domain Randomization Setup. Even though we design simulation tasks to be similar to the real world setup, domain randomization is necessary to be able to bridge the gap between the simulation and the real world. We apply visual domain randomization consisting of small random position, rotation, and FOV perturbations to the wrist camera, as well as lighting and color jitter alterations. We apply physical domain randomization where we randomize object sizes, object frictions and gripper closing speed. Furthermore, we apply additive isotropic Gaussian noise ($\sigma = 5$) to joint positions

in the proprioceptive state to ensure robustness to any joint position mismatches between simulation and real world setups. We *emphasize* that Squint is able to achieve fast training speed despite these aggressive randomizations.

Baselines. We compare our method, Squint, against the following competitive baselines: (1) **SAC**: an optimized implementation of Soft Actor Critic [24] for parallel simulators, with Squint’s tuned hyper parameters, but without Squint’s architectural differences. (2) **PPO**: an optimized implementation of Proximal Policy Optimization [63], the de facto standard for visual sim-to-real robotics due to its fast wall time training speed with parallel simulators. (3) **DrQ-v2**: Data Regularized Q-Learning, the sample efficiency standard for off-policy visual learning [78]. We note that we kept DrQ-v2 sequential with one environment, rather than parallelized, to stay true to its original implementation, and compare our method with the standard for off-policy visual learning. (4) **BC**: Behaviour Cloning [60, 3] from expert demonstrations, commonly used for distilling visual agents. (5) **DAgger**: Dataset Aggregation [61], a stronger imitation learning baseline than Behaviour Cloning, commonly used to train visual agents when there is access to the environment and the expert agent. We specifically focus on State-to-Visual DAgger [61, 54], where one trains an expert SAC state based agent and distills it into a visual actor for deployment.

VI. RESULTS

Overall Results. We display the *overall average* plot in Figure 5 and all *detailed results* in Figure 6, showcasing per-task breakdowns and the tables for both simulation and real world success rates. Our method, Squint, surpasses all baselines in terms of training wall-time speed, and achieves an average success rate of 96.1% over all tasks at the end of 15 minutes of training. On the real world results, our method achieves 91.3% success rate averaged over 80 trials for 8 tasks, surpassing baselines on the real robot setup.

TABLE I
SIMULATION SUCCESS RATES (%)

Task	Squint (Ours)	SAC	PPO	DrQ-v2	BC
Reach Cube	100.0 \pm 0.0	99.4 \pm 1.1	88.0 \pm 10.3	12.3 \pm 8.3	61.2 \pm 9.2
Reach Can	100.0 \pm 0.0	99.1 \pm 1.8	96.6 \pm 2.4	23.6 \pm 17.6	56.2 \pm 12.5
Lift Cube	99.8 \pm 0.4	98.1 \pm 2.4	92.8 \pm 4.5	0.0 \pm 0.0	46.2 \pm 3.1
Lift Can	98.8 \pm 2.5	95.4 \pm 3.5	96.2 \pm 4.7	0.0 \pm 0.0	53.8 \pm 12.9
Place Cube	97.5 \pm 3.1	99.1 \pm 1.7	29.0 \pm 33.8	0.0 \pm 0.0	38.8 \pm 8.3
Place Can	96.3 \pm 3.0	98.6 \pm 1.8	71.1 \pm 18.3	0.0 \pm 0.0	28.8 \pm 8.5
Stack Cube	95.0 \pm 6.1	97.7 \pm 1.6	4.9 \pm 9.7	0.0 \pm 0.0	26.2 \pm 9.2
Stack Can	81.2 \pm 8.8	18.7 \pm 23.2	3.0 \pm 6.1	0.0 \pm 0.0	23.8 \pm 13.3
All Tasks	96.1\pm1.6	88.3\pm3.4	60.2\pm4.0	4.5\pm2.9	41.9\pm4.2

TABLE II
REAL-WORLD SUCCESS RATES

Task	Squint (Ours)	SAC	PPO	DrQ-v2	BC
Reach Cube	10/10	10/10	7/10	4/10	8/10
Reach Can	10/10	10/10	10/10	4/10	7/10
Lift Cube	10/10	10/10	6/10	0/10	6/10
Lift Can	9/10	9/10	7/10	0/10	6/10
Place Cube	10/10	8/10	9/10	0/10	7/10
Place Can	10/10	6/10	4/10	0/10	0/10
Stack Cube	8/10	6/10	3/10	0/10	2/10
Stack Can	6/10	6/10	4/10	0/10	2/10
Total	73/80	65/80	50/80	8/80	38/80
All Tasks	91.3%	81.3%	62.5%	10.0%	47.5%

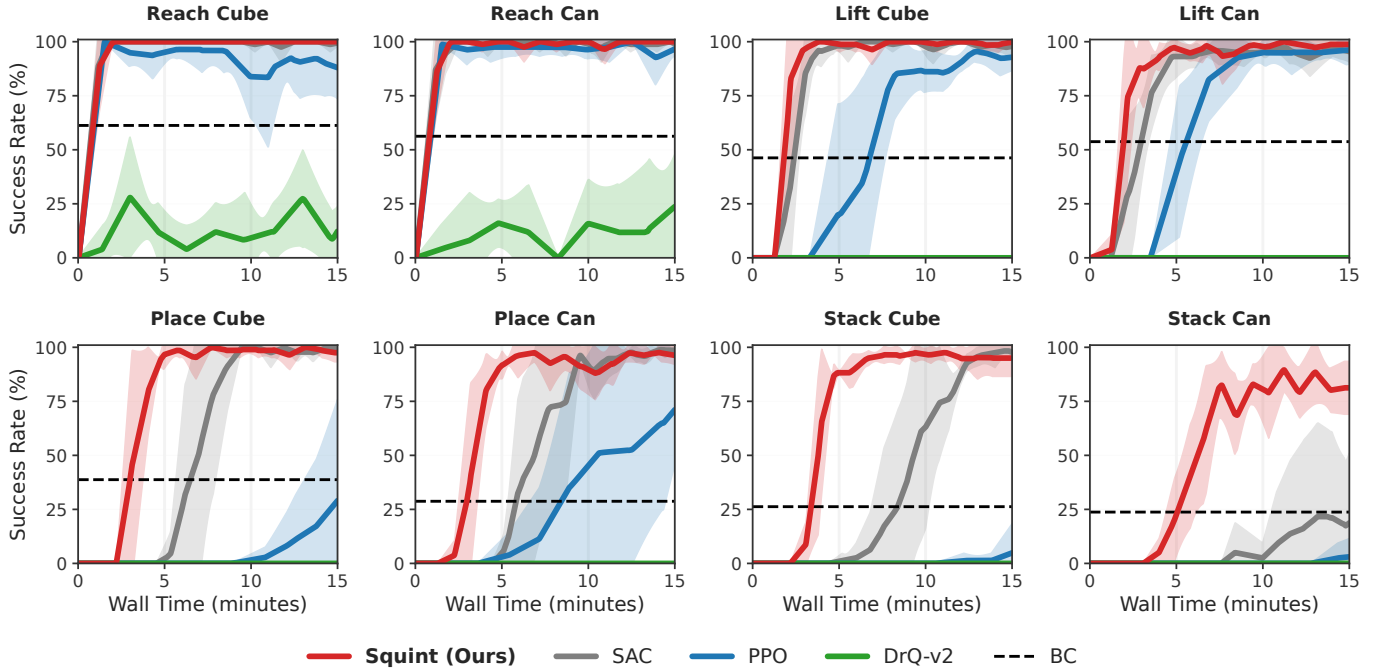


Fig. 6. **Detailed Results.** We train all methods for 15 minutes on all 8 tasks, and plot the results above. Mean Success Rates and 95% CI over 5 seeds. (Top Left) Simulation success rate table of all methods after 15 minutes. (Top Right) Real world success rate table over 10 trials for each task. (Bottom) Per-task success rate plots in simulation during training.

TABLE III
REAL WORLD SUCCESS - COMPARED WITH VISUAL DAGGER.

	Squint (Ours)	Visual DAgger
Total	73/80	53/80
Average	91.3%	66.3%

Comparison with Visual DAgger. We further compare our method with Visual DAgger agents that are distilled from SAC state experts and display the results in Figure 5. We include the time it takes to train SAC state experts as done in [54]. We find that Squint achieves similar training speed as the SAC state agent, and achieves higher success rate at the end of training than the State-to-Visual DAgger agent on our task

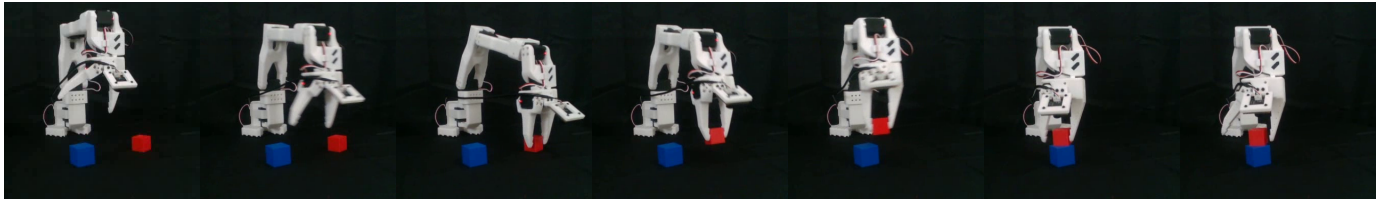
set. Furthermore, we deploy DAgger onto our real robot setup, showcasing the results in Table III, and we find that Squint outperforms DAgger’s success rate by 25% in the real world.

VII. DISCUSSION

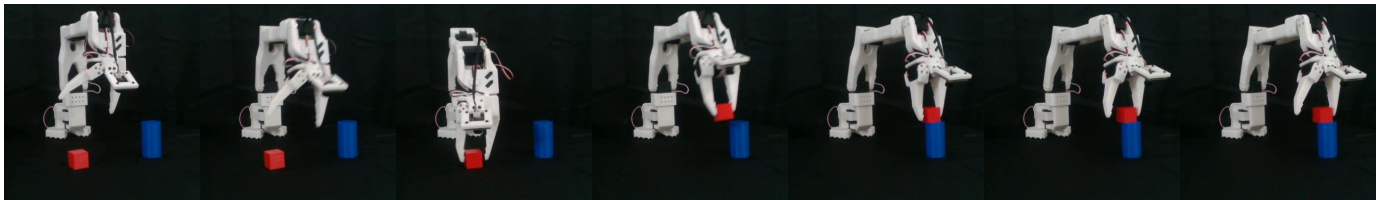
Quantitative Analysis. Based on simulation and real world results in Figure 6, we find that the real world results closely align with the simulation results. This indicates that the simulated environments provide a good test bed for measuring success in the real world. Our SAC baseline outperforms the other baselines, but falls short of Squint, due to its architectural limitations. Our PPO baseline doesn’t learn as fast as off-policy methods on the harder tasks of our task set, mainly due to the reuse of data that off-policy algorithms can leverage. Our DrQ-v2 baseline fails to learn, primarily due to it learning



(a) Place Can task.



(b) Stack Cube task.



(c) Stack Can task.

Fig. 7. **Qualitative Examples.** We show timesteps from left to right, and demonstrate successful deployment on our real world robot.

TABLE IV
REAL WORLD SUCCESS - VISUAL ROBUSTNESS.

	Squint (Ours)	Squint - No Color Jitter
Total	73/80	58/80
Average	91.3%	72.5%

from one environment only with heavy randomization, and doesn't benefit from the speed of parallelization. Our BC baseline learns, but is limited in performance due to the state distribution mismatch that DAgger can alleviate. While DAgger learns better, we find that it still falls short of Squint. Both BC and DAgger share a key limitation in our setting, which is learning from a state-based agent. Our task setup uses wrist cameras, which require active vision, and a different exploration movement than an all-seeing state agent would take. Overall, Squint shows promise as it accelerates wall-time speed of training deployable visual agents to the real world.

Qualitative Analysis. We display sample trajectories of Squint on the real SO-101 robot in Figure 7. The three trajectories consist of the three hardest tasks: PlaceCan, StackCube and StackCan.

Visual Robustness Analysis. Despite building a digital twin of the environment in simulation, visual reinforcement learning agents are brittle to changes in visuals that they haven't encountered before [1]. We found that even slight lighting changes in the real robot setup were degrading the performance of our deployed agent. We ablate removing color

jitter from our environment pipeline and evaluate it on the real robot setup. We display our results in Table IV, where we find that our agent's real world performance decreases by 18% on all tasks without the application of color jitter. We leave it to future work to integrate more visual robustness into the training pipeline.

VIII. CONCLUSION

Limitations and Opportunities. Building on this work, there are several limitations and promising directions that warrant further investigation:

- **Visual Robustness.** Visual reinforcement learning agents remains brittle to visual changes. While most prior works in off-policy learning focus on improving visual robustness under the sample efficiency axis, optimizing visual robustness under the wall-time axis presents an equally compelling objective—whether through visual augmentations [26, 1, 72, 48], pretrained encoders [81, 74, 9], or auxiliary representation learning objectives [6, 15].
- **Sample Efficiency.** Numerous advances in off-policy learning have yielded significant gains in sample efficiency [27, 42, 43, 20, 11, 57, 12]. Incorporating these methods into Squint while maximizing wall-time efficiency is a promising direction.
- **Gripper Design.** Despite the 5 DoF robot's remarkable capability for its price point, sim-to-real transfer for can grasping was challenging due to tipping and insufficient gripper friction. More adhesive [22] or alternative grip designs could mitigate this issue.

Algorithm 1 Squint: Pseudocode (distributional critic is omitted for simplicity)

```
1: Initialize encoder  $f_\psi$ , actor  $\pi_\phi$ , two critics  $Q_{\theta_1}, Q_{\theta_2}$ , entropy temperature  $\alpha$ , replay buffer  $\mathcal{B}$ 
2: Initialize target critics  $Q_{\bar{\theta}_1}, Q_{\bar{\theta}_2}$  with  $\bar{\theta}_1 \leftarrow \theta_1$  and  $\bar{\theta}_2 \leftarrow \theta_2$ 
3: for each environment step  $t$  do
4:   Observe  $(o_t^{\text{rgb}}, s_t^{\text{proprio}})$  and downsample image  $\tilde{o}_t = \text{DOWNSAMPLE}(o_t^{\text{rgb}})$ 
5:   Sample  $a_t \sim \pi_\phi(f_\psi(\tilde{o}_t), s_t^{\text{proprio}})$  and take action  $a_t$ 
6:   Observe next  $(o_{t+1}^{\text{rgb}}, s_{t+1}^{\text{proprio}})$  and reward  $r_t$ 
7:   Store transition  $\tau = (\tilde{o}_t, s_t^{\text{proprio}}, a_t, r_t, \text{DOWNSAMPLE}(o_{t+1}^{\text{rgb}}), s_{t+1}^{\text{proprio}})$  in  $\mathcal{B} \leftarrow \mathcal{B} \cup \{\tau\}$ 
8:   for  $j = 1$  to num_updates do
9:     Sample mini-batch  $B = \{\tau_k\}_{k=1}^{|B|}$  from  $\mathcal{B}$ 
10:    Encode observations:  $z_t \leftarrow f_\psi(\tilde{o}_t), z_{t+1} \leftarrow f_\psi(\tilde{o}_{t+1})$ 
11:    Compute target Q-value via average:
12:       $\tilde{a}_{t+1} \sim \pi_\phi(\cdot | z_{t+1}, s_{t+1}^{\text{proprio}})$ 
13:       $y = r_t + \frac{\gamma}{2} \sum_{i=1}^2 \left( Q_{\bar{\theta}_i}(z_{t+1}, s_{t+1}^{\text{proprio}}, \tilde{a}_{t+1}) - \alpha \log \pi_\phi(\tilde{a}_{t+1} | z_{t+1}, s_{t+1}^{\text{proprio}}) \right)$ 
14:    Update critic and encoder:
15:       $(\psi, \theta_i) \leftarrow (\psi, \theta_i) - \nabla_{(\psi, \theta_i)} \frac{1}{|B|} \sum_{\tau_k \in B} \left( Q_{\theta_i}(z_t, s_t^{\text{proprio}}, a_t) - y \right)^2$  for  $i \in \{1, 2\}$ 
16:    Update entropy temperature:
17:       $\alpha \leftarrow \alpha - \nabla_\alpha \frac{1}{|B|} \sum_{\tau_k \in B} (\mathcal{H}^{\text{target}} - \mathcal{H}(z_t, s_t^{\text{proprio}})) \cdot \alpha$ 
18:    if  $j \% \text{policy\_freq} == 0$  then
19:      Update actor:
20:         $z_t^{\text{sg}} \leftarrow \text{STOPGRAD}(z_t)$ 
21:         $\tilde{a}_t \sim \pi_\phi(\cdot | z_t^{\text{sg}}, s_t^{\text{proprio}})$ 
22:         $\phi \leftarrow \phi + \nabla_\phi \frac{1}{2|B|} \sum_{\tau_k \in B} \sum_{i=1}^2 \left( Q_{\theta_i}(z_t^{\text{sg}}, s_t^{\text{proprio}}, \tilde{a}_t) - \alpha \log \pi_\phi(\tilde{a}_t | z_t^{\text{sg}}, s_t^{\text{proprio}}) \right)$ 
23:      end if
24:      Update target critic  $\bar{\theta}_i \leftarrow \rho \bar{\theta}_i + (1 - \rho) \theta_i$  for  $i \in \{1, 2\}$ 
25:    end for
26: end for
```

- **Generalization.** While this work addresses single-task visual RL, natural extensions include multi-task [16, 76, 56], multi-view [82, 2, 45, 39], or multi-agent [79] settings as a step towards more generalist agents.
- **Privileged Training.** We formulated Squint as a symmetric visual based reinforcement learning agent for simplicity. Extending Squint to an asymmetric pipeline, where the critic could leverage privileged information [59, 33], could further speed up the learning.
- **Dataset Diversity.** Our work extensively evaluated the SO-101 task set in simulation and the real world. Evaluating and improving Squint on larger and diverse visual benchmarks is another promising direction [71, 80, 28].
- **Imitation Learning Limitations.** Imitation learning agents achieve suboptimal policies when given an active vision observation space and asked to imitate a state based agent. Future work could introduce imitation learning agents that address this limitation [33, 68].
- **Sim and Real Co-training.** While we train Squint policies purely from simulation, co-training with both parallel simulation and real world demonstrations could

prove a powerful way to bootstrap the learning [49].

Summary. Fast GPU-based parallel simulators have dramatically lowered the entry barrier for robot learning. In this work, we integrate the 5-DoF SO-101 robotic arm – a low-cost platform – into ManiSkill3, establishing 8 benchmark tasks with extensive domain randomization for sim-to-real transfer. We introduce Squint, an off-policy visual reinforcement learning algorithm that, through careful architectural design, hyperparameter tuning and image preprocessing, achieves superior wall-time efficiency and success rates compared to existing baselines on our proposed SO-101 Task Set. Squint trains on a single RTX 3090 GPU in under 15 minutes, producing policies ready for real-world deployment. We hope this work accelerates iteration cycles in robot learning, makes the field more accessible to researchers, and provides a strong foundation for future advances in visual reinforcement learning.

ACKNOWLEDGMENTS

This research has in part been sponsored by Kuwait University through a visiting fellow program. Their support is gratefully acknowledged.

REFERENCES

- [1] Abdulaziz Almuzairee, Nicklas Hansen, and Henrik I Christensen. A recipe for unbounded data augmentation in visual reinforcement learning. *arXiv preprint arXiv:2405.17416*, 2024.
- [2] Abdulaziz Almuzairee, Rohan Patil, Dwait Bhatt, and Henrik I Christensen. Merging and disentangling views in visual reinforcement learning for robotic manipulation. *arXiv preprint arXiv:2505.04619*, 2025.
- [3] Christopher G Atkeson and Stefan Schaal. Robot learning from demonstration. In *ICML*, volume 97, pages 12–20, 1997.
- [4] Jimmy Lei Ba, Jamie Ryan Kiros, and Geoffrey E Hinton. Layer normalization. *arXiv preprint arXiv:1607.06450*, 2016.
- [5] Philip J Ball, Laura Smith, Ilya Kostrikov, and Sergey Levine. Efficient online reinforcement learning with offline data. In *International Conference on Machine Learning*, pages 1577–1594. PMLR, 2023.
- [6] Sumeet Batra and Gaurav S Sukhatme. Zero shot generalization of vision-based rl without data augmentation. In *Forty-second International Conference on Machine Learning*, 2024.
- [7] Marc G Bellemare, Yavar Naddaf, Joel Veness, and Michael Bowling. The arcade learning environment: An evaluation platform for general agents. *Journal of artificial intelligence research*, 47:253–279, 2013.
- [8] Marc G Bellemare, Will Dabney, and Rémi Munos. A distributional perspective on reinforcement learning. In *International conference on machine learning*, pages 449–458. PMLR, 2017.
- [9] Alexandre Brown and Glen Berseth. Segdac: Improving visual reinforcement learning by extracting dynamic object-centric representations from pretrained vision models, 2026. URL <https://arxiv.org/abs/2508.09325>.
- [10] Remi Cadene, Simon Alibert, Alexander Soare, Quentin Gallouedec, Adil Zouitine, Steven Palma, Pepijn Kooijmans, Michel Aractingi, Mustafa Shukor, Dana Aubakirova, Martino Russi, Francesco Capuano, Caroline Pascal, Jade Choghari, Jess Moss, and Thomas Wolf. Lerobot: State-of-the-art machine learning for real-world robotics in pytorch. <https://github.com/huggingface/lerobot>, 2024.
- [11] Roger Creus Castanyer, Johan Obando-Ceron, Lu Li, Pierre-Luc Bacon, Glen Berseth, Aaron Courville, and Pablo Samuel Castro. Stable gradients for stable learning at scale in deep reinforcement learning. *arXiv preprint arXiv:2506.15544*, 2025.
- [12] Wei-Di Chang, Mikael Henaff, Brandon Amos, Gregory Dudek, and Scott Fujimoto. The surprising difficulty of search in model-based reinforcement learning. *arXiv preprint arXiv:2601.21306*, 2026.
- [13] Jack Collins, Shelvin Chand, Anthony Vanderkop, and David Howard. A review of physics simulators for robotic applications. *IEEE Access*, 9:51416–51431, 2021.
- [14] Pierluca D’Oro, Max Schwarzer, Evgenii Nikishin, Pierre-Luc Bacon, Marc G Bellemare, and Aaron Courville. Sample-efficient reinforcement learning by breaking the replay ratio barrier. In *The Eleventh International Conference on Learning Representations*, 2023. URL <https://openreview.net/forum?id=OpC-9aBBVJe>.
- [15] Ayoub Echchahed and Pablo Samuel Castro. A survey of state representation learning for deep reinforcement learning. *arXiv preprint arXiv:2506.17518*, 2025.
- [16] Lasse Espeholt, Hubert Soyer, R. Munos, K. Simonyan, V. Mnih, Tom Ward, Yotam Doron, Vlad Firoiu, et al. Impala: Scalable distributed deep-rl with importance weighted actor-learner architectures. *ArXiv*, abs/1802.01561, 2018.
- [17] Chelsea Finn, Xin Yu Tan, Yan Duan, Trevor Darrell, Sergey Levine, and Pieter Abbeel. Learning visual feature spaces for robotic manipulation with deep spatial autoencoders. *arXiv preprint arXiv:1509.06113*, 25(2), 2015.
- [18] Scott Fujimoto, H. V. Hoof, and D. Meger. Addressing function approximation error in actor-critic methods. *ArXiv*, abs/1802.09477, 2018.
- [19] Scott Fujimoto, Herke Hoof, and David Meger. Addressing function approximation error in actor-critic methods. In *International conference on machine learning*, pages 1587–1596. PMLR, 2018.
- [20] Scott Fujimoto, Pierluca D’Oro, Amy Zhang, Yuandong Tian, and Michael Rabbat. Towards general-purpose model-free reinforcement learning. *arXiv preprint arXiv:2501.16142*, 2025.
- [21] Matteo Gallici, Mattie Fellows, Benjamin Ellis, Bartomeu Pou, Ivan Masmitja, Jakob Nicolaus Foerster, and Mario Martin. Simplifying deep temporal difference learning. *arXiv preprint arXiv:2407.04811*, 2024.
- [22] Paul Glick, Srinivasan A Suresh, Donald Ruffatto, Mark Cutkosky, Michael T Tolley, and Aaron Parness. A soft robotic gripper with gecko-inspired adhesive. *IEEE Robotics and Automation Letters*, 3(2):903–910, 2018.
- [23] Jiayuan Gu, Fanbo Xiang, Xuanlin Li, Zhan Ling, Xiqiang Liu, Tongzhou Mu, Yihe Tang, Stone Tao, Xinyue Wei, Yunchao Yao, et al. Maniskill2: A unified benchmark for generalizable manipulation skills. *arXiv preprint arXiv:2302.04659*, 2023.
- [24] Tuomas Haarnoja, Aurick Zhou, Pieter Abbeel, and Sergey Levine. Soft actor-critic: Off-policy maximum entropy deep reinforcement learning with a stochastic actor. *arXiv preprint arXiv:1801.01290*, 2018.
- [25] Danijar Hafner, Jurgis Pasukonis, Jimmy Ba, and Timothy Lillicrap. Mastering diverse domains through world models. *arXiv preprint arXiv:2301.04104*, 2023.
- [26] Nicklas Hansen, Hao Su, and Xiaolong Wang. Stabilizing deep q-learning with convnets and vision transformers under data augmentation. In *Annual Conference on Neural Information Processing Systems (NeurIPS)*, 2021.

- [27] Nicklas Hansen, Hao Su, and Xiaolong Wang. TD-MPC2: Scalable, robust world models for continuous control. In *International Conference on Learning Representations (ICLR)*, 2024.
- [28] Nicklas Hansen, Hao Su, and Xiaolong Wang. Learning massively multitask world models for continuous control. *arXiv preprint arXiv:2511.19584*, 2025.
- [29] H. V. Hasselt, A. Guez, and D. Silver. Deep reinforcement learning with double q-learning. In *Aaai*, 2016.
- [30] Nicolas Heess, Dhruva Tb, Srinivasan Sriram, Jay Lemmon, Josh Merel, Greg Wayne, Yuval Tassa, Tom Erez, Ziyu Wang, SM Eslami, et al. Emergence of locomotion behaviours in rich environments. *arXiv preprint arXiv:1707.02286*, 2017.
- [31] Yuenan Hou, Lifeng Liu, Qing Wei, Xudong Xu, and Chunlin Chen. A novel ddpg method with prioritized experience replay. In *2017 IEEE international conference on systems, man, and cybernetics (SMC)*, pages 316–321. IEEE, 2017.
- [32] Kyle Hsu, Moo Jin Kim, Rafael Rafailov, Jiajun Wu, and Chelsea Finn. Vision-based manipulators need to also see from their hands. *arXiv preprint arXiv:2203.12677*, 2022.
- [33] Edward S Hu, James Springer, Oleh Rybkin, and Dinesh Jayaraman. Privileged sensing scaffolds reinforcement learning. *arXiv preprint arXiv:2405.14853*, 2024.
- [34] Shengyi Huang, Rousslan Fernand Julien Dossa, Chang Ye, Jeff Braga, Dipam Chakraborty, Kinal Mehta, and João G.M. Araújo. Cleanrl: High-quality single-file implementations of deep reinforcement learning algorithms. *Journal of Machine Learning Research*, 23(274): 1–18, 2022. URL <http://jmlr.org/papers/v23/21-1342.html>.
- [35] Jemin Hwangbo, Joonho Lee, Alexey Dosovitskiy, Dario Bellicoso, Vassilios Tsounis, Vladlen Koltun, and Marco Hutter. Learning agile and dynamic motor skills for legged robots. *Science Robotics*, 4(26):eaau5872, 2019.
- [36] Leslie Pack Kaelbling, Michael L. Littman, and Anthony R. Cassandra. Planning and acting in partially observable stochastic domains. *Artificial Intelligence*, 1998.
- [37] Dmitry Kalashnikov, Alex Irpan, Peter Pastor, Julian Ibarz, Alexander Herzog, Eric Jang, Deirdre Quillen, Ethan Holly, Mrinal Kalakrishnan, Vincent Vanhoucke, et al. Qt-opt: Scalable deep reinforcement learning for vision-based robotic manipulation. *arXiv preprint arXiv:1806.10293*, 2018.
- [38] Elia Kaufmann, Leonard Bauersfeld, Antonio Loquercio, Matthias Müller, Vladlen Koltun, and Davide Scaramuzza. Champion-level drone racing using deep reinforcement learning. *Nat.*, 620(7976):982–987, 2023. doi: 10.1038/S41586-023-06419-4. URL <https://doi.org/10.1038/s41586-023-06419-4>.
- [39] Sunghwan Kim, Woojeh Chung, Zhirui Dai, Dwait Bhatt, Arth Shukla, Hao Su, Yulun Tian, and Nikolay Atanasov. Seeing the bigger picture: 3d latent mapping for mobile manipulation policy learning. *arXiv preprint arXiv:2510.03885*, 2025.
- [40] Ilya Kostrikov, Denis Yarats, and Rob Fergus. Image augmentation is all you need: Regularizing deep reinforcement learning from pixels. *arXiv preprint arXiv:2004.13649*, 2020.
- [41] Michael Laskin, Kimin Lee, Adam Stooke, Lerrel Pinto, Pieter Abbeel, and Aravind Srinivas. Reinforcement learning with augmented data. *arXiv preprint arXiv:2004.14990*, 2020.
- [42] Hojoon Lee, Dongyoon Hwang, Donghu Kim, Hyunseung Kim, Jun Jet Tai, Kaushik Subramanian, Peter R Wurman, Jaegul Choo, Peter Stone, and Takuma Seno. Simba: Simplicity bias for scaling up parameters in deep reinforcement learning. *arXiv preprint arXiv:2410.09754*, 2024.
- [43] Hojoon Lee, Youngdo Lee, Takuma Seno, Donghu Kim, Peter Stone, and Jaegul Choo. Hyperspherical normalization for scalable deep reinforcement learning. *arXiv preprint arXiv:2502.15280*, 2025.
- [44] Zechu Li, Tao Chen, Zhang-Wei Hong, Anurag Ajay, and Pulkit Agrawal. Parallel q-learning: Scaling off-policy reinforcement learning under massively parallel simulation. In *International Conference on Machine Learning*, pages 19440–19459. PMLR, 2023.
- [45] Zheng Li, Pei Qu, Yufei Jia, Shihui Zhou, Haizhou Ge, Jiahang Cao, Jinni Zhou, Guyue Zhou, and Jun Ma. Manivid-3d: Generalizable view-invariant reinforcement learning for robotic manipulation via disentangled 3d representations. *arXiv preprint arXiv:2509.11125*, 2025.
- [46] Jacky Liang, Viktor Makoviychuk, Ankur Handa, Nuttapong Chentanez, Miles Macklin, and Dieter Fox. Gpu-accelerated robotic simulation for distributed reinforcement learning. In *Conference on Robot Learning*, pages 270–282. PMLR, 2018.
- [47] Timothy P Lillicrap, Jonathan J Hunt, Alexander Pritzel, Nicolas Heess, Tom Erez, Yuval Tassa, David Silver, and Daan Wierstra. Continuous control with deep reinforcement learning. *arXiv preprint arXiv:1509.02971*, 2015.
- [48] Guozheng Ma, Zhen Wang, Zhecheng Yuan, Xueqian Wang, Bo Yuan, and Dacheng Tao. A comprehensive survey of data augmentation in visual reinforcement learning. *International Journal of Computer Vision*, 133(10):7368–7405, 2025.
- [49] Abhiram Maddukuri, Zhenyu Jiang, Lawrence Yunliang Chen, Soroush Nasiriany, Yuqi Xie, Yu Fang, Wenqi Huang, Zu Wang, Zhenjia Xu, Nikita Chernyadev, et al. Sim-and-real co-training: A simple recipe for vision-based robotic manipulation. *arXiv preprint arXiv:2503.24361*, 2025.
- [50] Viktor Makoviychuk, Lukasz Wawrzyniak, Yunrong Guo, Michelle Lu, Kier Storey, Miles Macklin, David Hoeller, Nikita Rudin, Arthur Allshire, Ankur Handa, et al. Isaac gym: High performance gpu-based physics simulation for robot learning. *arXiv preprint arXiv:2108.10470*, 2021.

- [51] Volodymyr Mnih, Koray Kavukcuoglu, David Silver, Alex Graves, Ioannis Antonoglou, Daan Wierstra, and Martin Riedmiller. Playing atari with deep reinforcement learning. *arXiv preprint arXiv:1312.5602*, 2013.
- [52] Volodymyr Mnih, Koray Kavukcuoglu, David Silver, Andrei A Rusu, Joel Veness, Marc G Bellemare, Alex Graves, Martin Riedmiller, Andreas K Fidjeland, Georg Ostrovski, et al. Human-level control through deep reinforcement learning. *nature*, 518(7540):529–533, 2015.
- [53] Tongzhou Mu, Zhan Ling, Fanbo Xiang, Derek Yang, Xuanlin Li, Stone Tao, Zhiao Huang, Zhiwei Jia, and Hao Su. Maniskill: Generalizable manipulation skill benchmark with large-scale demonstrations. *arXiv preprint arXiv:2107.14483*, 2021.
- [54] Tongzhou Mu, Zhaoyang Li, Stanisław Wiktor Strzelecki, Xiu Yuan, Yunchao Yao, Litian Liang, and Hao Su. When should we prefer state-to-visual dagger over visual reinforcement learning? *Proceedings of the AAAI Conference on Artificial Intelligence*, 39(14):14637–14645, 2025.
- [55] Michal Nauman, Mateusz Ostaszewski, Krzysztof Jankowski, Piotr Miłoś, and Marek Cygan. Bigger, regularized, optimistic: scaling for compute and sample efficient continuous control. *Advances in neural information processing systems*, 37:113038–113071, 2024.
- [56] Michal Nauman, Marek Cygan, Carmelo Sferrazza, Aviral Kumar, and Pieter Abbeel. Bigger, regularized, categorical: High-capacity value functions are efficient multi-task learners. *arXiv preprint arXiv:2505.23150*, 2025.
- [57] Johan Obando-Ceron, Walter Mayor, Samuel Lavoie, Scott Fujimoto, Aaron Courville, and Pablo Samuel Castro. Simplicial embeddings improve sample efficiency in actor-critic agents. *arXiv preprint arXiv:2510.13704*, 2025.
- [58] Adam Paszke, Sam Gross, Francisco Massa, Adam Lerer, James Bradbury, Gregory Chanan, Trevor Killeen, Zeming Lin, Natalia Gimelshein, Luca Antiga, et al. Pytorch: An imperative style, high-performance deep learning library. *Advances in neural information processing systems*, 32, 2019.
- [59] Lerrel Pinto, Marcin Andrychowicz, Peter Welinder, Wojciech Zaremba, and Pieter Abbeel. Asymmetric actor critic for image-based robot learning. *arXiv preprint arXiv:1710.06542*, 2017.
- [60] Dean A Pomerleau. Alvin: An autonomous land vehicle in a neural network. *Advances in neural information processing systems*, 1, 1988.
- [61] Stéphane Ross, Geoffrey Gordon, and Drew Bagnell. A reduction of imitation learning and structured prediction to no-regret online learning. In *Proceedings of the fourteenth international conference on artificial intelligence and statistics*, pages 627–635. JMLR Workshop and Conference Proceedings, 2011.
- [62] Tom Schaul, John Quan, Ioannis Antonoglou, and David Silver. Prioritized experience replay. *arXiv preprint arXiv:1511.05952*, 2015.
- [63] John Schulman, Filip Wolski, Prafulla Dhariwal, Alec Radford, and Oleg Klimov. Proximal policy optimization algorithms. *arXiv preprint arXiv:1707.06347*, 2017.
- [64] Younggyo Seo, Carmelo Sferrazza, Juyue Chen, Guanya Shi, Rocky Duan, and Pieter Abbeel. Learning sim-to-real humanoid locomotion in 15 minutes. *arXiv preprint arXiv:2512.01996*, 2025.
- [65] Younggyo Seo, Carmelo Sferrazza, Haoran Geng, Michal Nauman, Zhao-Heng Yin, and Pieter Abbeel. Fasttd3: Simple, fast, and capable reinforcement learning for humanoid control. *arXiv preprint arXiv:2505.22642*, 2025.
- [66] Carmelo Sferrazza, Dun-Ming Huang, Xingyu Lin, Youngwoon Lee, and Pieter Abbeel. Humanoidbench: Simulated humanoid benchmark for whole-body locomotion and manipulation. *arXiv preprint arXiv:2403.10506*, 2024.
- [67] Arth Shukla. Speeding up sac with massively parallel simulation. <https://arthshukla.substack.com>, Mar 2025. URL <https://arthshukla.substack.com/p/speeding-up-sac-with-massively-parallel>.
- [68] Yuda Song, Dhruv Rohatgi, Aarti Singh, and J Andrew Bagnell. To distill or decide? understanding the algorithmic trade-off in partially observable reinforcement learning. *arXiv preprint arXiv:2510.03207*, 2025.
- [69] Aravind Srinivas, Michael Laskin, and Pieter Abbeel. Curl: Contrastive unsupervised representations for reinforcement learning. *arXiv preprint arXiv:2004.04136*, 2020.
- [70] Stone Tao, Fanbo Xiang, Arth Shukla, Yuzhe Qin, Xander Hinrichsen, Xiaodi Yuan, Chen Bao, Xinsong Lin, Yulin Liu, Tse-kai Chan, et al. Maniskill3: Gpu parallelized robotics simulation and rendering for generalizable embodied ai. *arXiv preprint arXiv:2410.00425*, 2024.
- [71] Yuval Tassa, Yotam Doron, Alistair Muldal, Tom Erez, Yazhe Li, Diego de Las Casas, David Budden, Abbas Abdolmaleki, Josh Merel, Andrew Lefrancq, et al. Deepmind control suite. *arXiv preprint arXiv:1801.00690*, 2018.
- [72] Eugene Teoh, Sumit Patidar, Xiao Ma, and Stephen James. Green screen augmentation enables scene generalisation in robotic manipulation. *arXiv preprint arXiv:2407.07868*, 2024.
- [73] Josh Tobin, Rachel Fong, Alex Ray, Jonas Schneider, Wojciech Zaremba, and Pieter Abbeel. Domain randomization for transferring deep neural networks from simulation to the real world. In *2017 IEEE/RSJ international conference on intelligent robots and systems (IROS)*, pages 23–30. IEEE, 2017.
- [74] Ziyu Wang, Yanjie Ze, Yifei Sun, Zhecheng Yuan, and Huazhe Xu. Generalizable visual reinforcement learning with segment anything model. *arXiv preprint arXiv:2312.17116*, 2023.

- [75] Christopher JCH Watkins and Peter Dayan. Q-learning. *Machine learning*, 8:279–292, 1992.
- [76] Charles Xu, Qiyang Li, Jianlan Luo, and Sergey Levine. Rldg: Robotic generalist policy distillation via reinforcement learning. *arXiv preprint arXiv:2412.09858*, 2024.
- [77] Denis Yarats, Amy Zhang, Ilya Kostrikov, Brandon Amos, Joelle Pineau, and Rob Fergus. Improving sample efficiency in model-free reinforcement learning from images, 2019.
- [78] Denis Yarats, Rob Fergus, Alessandro Lazaric, and Lerrel Pinto. Mastering visual continuous control: Improved data-augmented reinforcement learning. *arXiv preprint arXiv:2107.09645*, 2021.
- [79] Chao Yu, Akash Velu, Eugene Vinitsky, Jiaxuan Gao, Yu Wang, Alexandre Bayen, and Yi Wu. The surprising effectiveness of ppo in cooperative multi-agent games. *Advances in neural information processing systems*, 35: 24611–24624, 2022.
- [80] Tianhe Yu, Deirdre Quillen, Zhanpeng He, Ryan Julian, Karol Hausman, Chelsea Finn, and Sergey Levine. Meta-world: A benchmark and evaluation for multi-task and meta reinforcement learning. In *Conference on robot learning*, pages 1094–1100. PMLR, 2020.
- [81] Zhecheng Yuan, Zhengrong Xue, Bo Yuan, Xueqian Wang, Yi Wu, Yang Gao, and Huazhe Xu. Pre-trained image encoder for generalizable visual reinforcement learning. *Advances in Neural Information Processing Systems*, 35:13022–13037, 2022.
- [82] Zhecheng Yuan, Tianming Wei, Shuiqi Cheng, Gu Zhang, Yuanpei Chen, and Huazhe Xu. Learning to manipulate anywhere: A visual generalizable framework for reinforcement learning. *arXiv preprint arXiv:2407.15815*, 2024.
- [83] Kevin Zakka, Baruch Tabanpour, Qiayuan Liao, Mustafa Haiderbhai, Samuel Holt, Jing Yuan Luo, Arthur Allshire, Erik Frey, Koushil Sreenath, Lueder A Kahrs, et al. Mujoco playground. *arXiv preprint arXiv:2502.08844*, 2025.
- [84] Yuke Zhu, Josiah Wong, Ajay Mandlekar, Roberto Martín-Martín, Abhishek Joshi, Soroush Nasiriany, and Yifeng Zhu. robosuite: A modular simulation framework and benchmark for robot learning. *arXiv preprint arXiv:2009.12293*, 2020.
- [85] Ziwen Zhuang, Zipeng Fu, Jianren Wang, Christopher Atkeson, Soeren Schwertfeger, Chelsea Finn, and Hang Zhao. Robot parkour learning. *arXiv preprint arXiv:2309.05665*, 2023.